Viewing Corridors as Right Parallelepipeds for Vision-Based Vehicle Localization

Zhi-Fang Yang and Wen-Hsiang Tsai, *Senior Member, IEEE*

***Abstract*—An approach to vision-based vehicle localization by viewing corridors as a combination of right parallelepipeds is proposed. The objective is to derive the orientation and lateral position of a vehicle in a right parallelepiped corridor. These two kinds of information are all that is needed for vehicles to navigate safely in a right parallelepiped corridor. This approach offers low hardware cost and simple computation. Only one camera mounted on the vehicle is needed, and analytic formulas are derived for computing the vehicle location. The information source is the corridor ceiling. Two orthogonal sets of parallel lines on the corridor ceiling are used to detect the vanishing line of the ceiling. An equation is developed to derive the vehicle orientation by utilizing the detected vanishing line. Also, based on the observation of the variation of image line slopes when we move laterally, another equation is established to evaluate the relative lateral position of the vehicle by utilizing the line slope of the ceiling line pointing forward. Experiments have been conducted, and acceptable vehicle localization results have been obtained, to prove the feasibility of the proposed approach.**

***Index Terms*—Ceiling, corridor, line slope, right parallelepiped, vanishing line, vehicle localization.**

I. Introduction

AUTONOMOUS vehicle navigation is a multidisciplinary and demanding field. Among the research topics in this field, the localization problem [1]–[7] is critical to any autonomous vehicle. To complete this task, the orientation and position of a vehicle with respect to the environment should be obtained. Other research topics include obstacle avoidance, guidance, control, path planning/replanning, calibration, tracking, and so on [8]–[14].

There are two kinds of vision-based approaches to solving the localization problem: the map approach [1]–[4] and the landmark approach [5]–[7]. The first kind of approach requires a detailed map of the environment. The features extracted from sensor data are matched with the features in the map to estimate the vehicle location. A difficulty here is the establishment of the correspondence between sensor data and the map. The second kind of approach takes advantage of landmarks in the environment, for example, a door or a corner. Strategies for landmark detection are needed. The knowledge of landmark locations is utilized to locate the vehicle. A dead-reckoning system is usually required to provide information for localization between landmarks. Although this method does not have the severe correspondence problem like the map-based solution does, it suffers from the localization errors between landmarks produced by the dead-reckoning system.

Vision-based vehicle localization between landmarks with the aim of low hardware cost and fast computation is the interest of this paper. Emphasis is placed on the study of vehicle localization in the corridor environment. The motivation is as follows. Vehicle localization inaccuracy accumulated by dead reckoning is inevitable when a vehicle navigates between landmarks. In particular, when the vehicle navigates in corridors with crossings as landmarks, the distance between two crossings is usually long. Hence, in this paper, an approach to vision-based localization between landmarks in the corridor environment is proposed to replace the dead-reckoning system. Only vision sensors are used to achieve low hardware cost. They are utilized to acquire images at the less occluded scene to avoid being interrupted by obstacles in corridors. In the mean time, vision techniques with simple computations are developed based on viewing corridors as a combination of right parallelepipeds.

The connecting part of adjacent corridors is a crossing. The long narrow passage between every two crossings is generally in the shape of a right parallelepiped. The proposed approach is designed to solve the localization problem in the right parallelepiped corridor. Corridor ceilings are utilized as the visual information source. Such a selection is based on two good properties of corridor ceilings: seldom being disturbed and usually having uniform patterns. Two sets of parallel lines on the ceiling are utilized to compute the location information. Such ceiling patterns are quite common in modern buildings. The orientation and the lateral position of the vehicle in the right parallelepiped are computed. The forward position of the vehicle in the right parallelepiped is not necessary, since landmarks provide sufficient information for this. Thus, this approach can be used to cooperate with landmark methods to achieve autonomous vehicle guidance and navigation in corridors.

The proposed approach is described briefly as follows. A single camera mounted on the vehicle is employed as the only sensor. Two orthogonal sets of parallel lines on the ceiling in the acquired images are extracted. The vanishing line of the ceiling is detected by utilizing the vanishing points of these two sets of parallel lines. The orientation of the vehicle is computed via the line direction of this vanishing line. The lateral position of the vehicle is determined by utilizing the line slopes of the ceiling lines with respect to the vehicle. It is shown that different lateral positions of the vehicle produce different line slopes of one ceiling line. A formula is derived

Manuscript received August 20, 1997; revised August 25, 1998. Abstract published on the Internet March 1, 1999. This work was supported by the National Science Council, Taiwan, R.O.C., under Grant NSC-84-2213-E009-122.

The authors are with the Department of Computer and Information Science, National Chiao Tung University, Hsinchu, Taiwan, 30050, R.O.C. (e-mail: whtsai@cis.nctu.edu.tw).

Publisher Item Identifier S 0278-0046(99)04148-9.

to calculate the lateral position of the vehicle by the line slopes of the ceiling lines pointing forward.

One of the main ideas of this paper is the use of the vanishing-point concept in determining the orientation of the vehicle. Reference [19] is a related work, where a camera calibration technique was developed by using a vanishing-point concept. The vanishing points of two orthogonal sets of parallel lines on a two-dimensional (2-D) grid paper are utilized to determine the rotation matrix. The rotation matrix is evaluated in the form of a 3×3 matrix with nine unknowns. Theoretically, the inner product of these two vanishing points should be zero. Without this property, the vectors in the computed matrix are not orthogonal and it cannot be called a rotation matrix. In order to fit this constraint, the values of the inspected vanishing points are utilized in an error estimator which adjusts parameters determining the unknowns of the rotation matrix. Advanced statistical methods are used to achieve subpixel accuracy. The goal of this calibration technique is to use it for precision measurement with the same accuracy as that of a contact instrument (e.g., micrometer, caliper, or height gage). However, in this paper, the main interest is vehicle localization in corridors. And the vanishing-point concept is utilized to derive the vehicle orientation. Furthermore, in this paper, the orientation of the vehicle is treated as three separate angles: pan, tilt, and swing. Since the three rotational angles rather than the whole rotation matrix are considered, it is not necessary for the two sets of inspected parallel lines to be orthogonal. No statistical methods are required to adjust the inspected values. Only the computation of the analytic formulas is needed.

The remainder of this paper is organized as follows. The descriptions of the concept of viewing corridors as right parallelepipeds, the coordinate systems, and the transformations between them are described in Section II. Section III includes a discussion on the use of vanishing lines for calculating the orientation of the vehicle. Section IV includes the description of detecting the lateral position of the vehicle. Experimental results and discussions can be found in Section V, and some conclusions are given in Section VI.

II. Viewing Corridors as Right Parallelepipeds and Corresponding Coordinate Systems

The viewpoint of regarding corridors as a combination of right parallelepipeds indicates which information is necessary to solve the localization problem and provides a clue to dividing the problem into two subtasks. It also facilitates coordinate system setup in this study.

A. Viewing Corridors as Combination of Right Parallelepipeds

Imagine the process of walking in corridors. The walker moves forward in a corridor which is usually in the shape of a right parallelepiped, encounters a crossing and changes direction, enters a new right parallelepiped and moves forward, encounters a crossing and changes direction, enters yet another new right parallelepiped and moves forward, and so on, until the walker stops.

Orientation and lateral position information is all that is needed for a person to walk safely inside a right parallelepiped corridor; nothing else is required. Such an observation matches our common experience that a walker in a corridor generally just keeps moving in a straight line, and notices the crossing in front. Such an observation can be applied to the vehicle localization problem. To be autonomous, the vehicle should self-decide its orientation and lateral position in right parallelepiped corridors. The crossings can be treated as landmarks which provide information for the forward position of the vehicle. Accordingly, the vehicle localization problem in a right parallelepiped can be divided into two subtasks; one is to derive the vehicle orientation, and the other is to derive the lateral vehicle position.

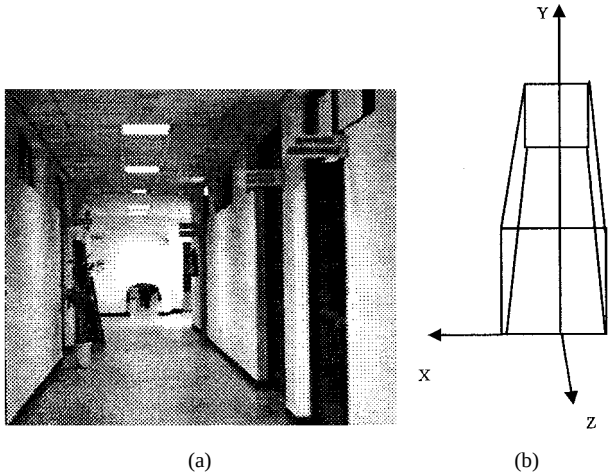

Fig. 1. Corridor representation. (a) Corridor image. (b) Global coordinate system.

B. Coordinate Systems and Transformations

The coordinate systems and the transformations between them used in this paper are described now. Viewing a corridor as a right parallelepiped sets up the global coordinate system (GCS), denoted as x–y–z, as shown in Fig. 1. The three main axes are parallel to the three main edges of the right parallelepiped, respectively. The camera mounted on the vehicle is attached with a camera coordinate system (CCS), denoted as x'–y'–z'. The camera lens center points to the origin of the CCS. The corresponding image plane (ICS) is denoted as u–v. The relation among the three coordinate systems is illustrated in Fig. 2.

The coordinate transformation from a point (x, y, z) in the GCS to a point (x', y', z') in the CCS can be written as

$$(x', y', z') = (x - x_d, y - y_d, z - z_d)\mathbf{T}_\phi \mathbf{T}_\theta \mathbf{T}_\psi \qquad (1)$$

where

$$\mathbf{T}_\phi = \begin{bmatrix} \cos\phi & 0 & -\sin\phi \\ 0 & 1 & 0 \\ \sin\phi & 0 & \cos\phi \end{bmatrix}$$

$$\mathbf{T}_\theta = \begin{bmatrix} 1 & 0 & 0 \\ 0 & \cos\theta & \sin\theta \\ 0 & -\sin\theta & \cos\theta \end{bmatrix}$$

$$\mathbf{T}_\psi = \begin{bmatrix} \cos\psi & \sin\psi & 0 \\ -\sin\psi & \cos\psi & 0 \\ 0 & 0 & 1 \end{bmatrix}.$$

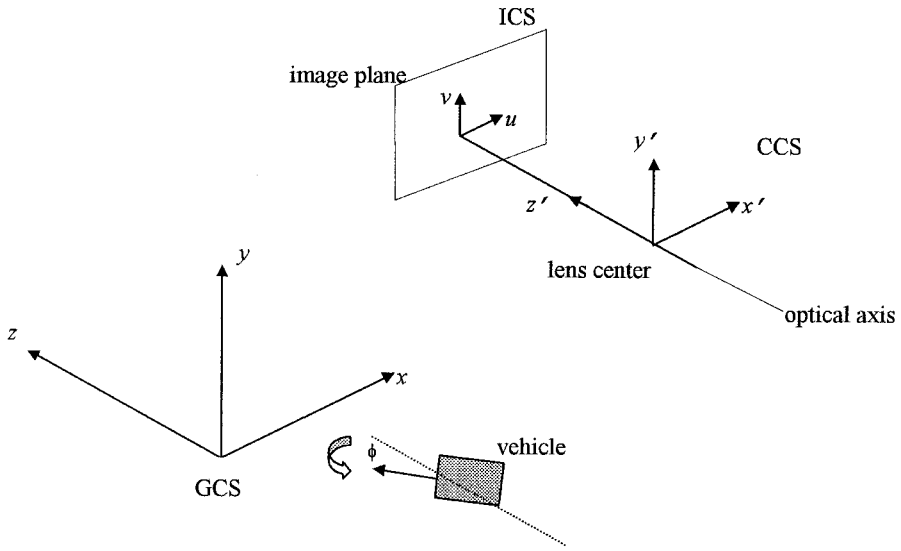

Fig. 2. The CCS x'–y'–z', the ICS u–v, and the GCS x–y–z.

ϕ, θ, and ψ are the pan, tilt, and swing angles of the CCS, respectively, with respect to the GCS, and (x_d, y_d, z_d) is the translation vector from the origin of the GCS to the origin of the CCS. The three orientation angles and the translation vector are all known in advance by a calibration process [15].

Also, the transformation of line directions from the GCS to the CCS is needed. The transformation from the direction of a line in the GCS, denoted as (d_x, d_y, d_z), to the direction of a line in the CCS, denoted as $(d_{x'}, d_{y'}, d_{z'})$, is as follows:

$$(d_{x'}, d_{y'}, d_{z'}) = (d_x, d_y, d_z)\mathbf{T}_\phi\mathbf{T}_\theta\mathbf{T}_\psi. \tag{2}$$

According to the perspective transformation principle [16], the image point (u, v) in the ICS of the point (x', y', z') in the CCS is written as

$$(u, v) = f\left(\frac{x'}{z'}, \frac{y'}{z'}\right) \tag{3}$$

where f is the focal length.

In this paper, the orientation of the vehicle is finally derived via the computed pan angle of the CCS with respect to the GCS. Here, we define ϕ_v to be the orientation of the vehicle, ϕ the computed pan angle of the CCS with respect to the GCS, and ϕ_{vc} the pan angle of the vehicle with respect to the CCS. Notice that ϕ_{vc} is known by a calibration technique [15] in advance. Then, the transformation can be written as follows:

$$\phi_v = \phi + \phi_{vc}. \tag{4}$$

For the same situation described above, the lateral position of the vehicle is derived via the computed lateral position of the CCS with respect to the GCS, and we define x_v to be the lateral position of the vehicle, Δx_c the computed lateral position of the CCS with respect to the GCS, and x_{vc} the lateral position of the vehicle with respect to the CCS defined as the location of the middle point of the rod connecting the two front wheels. The value of x_{vc} is known by measurement in advance. Then, the translation formula is as follows:

$$x_v = \Delta x_c + x_{vc}. \tag{5}$$

III. Detection of Vehicle Orientation from Vanishing Line Information in Corridor Ceiling

The orientation of the vehicle in the right parallelepiped corridor is derived via the vanishing line of the corridor ceiling. A formula describing the line direction of the vanishing line of a corridor ceiling in the ICS is derived first. Then, we describe how the vanishing line of the corridor ceiling in an acquired image is detected. The detected results and the derived formula can be used to set up an equation. Solving the equation, we can get the orientation of the vehicle.

A. Concept of Vanishing Line

One reason why vanishing lines play an important role in computer vision is that certain three-dimensional (3-D) information can be recovered from the vanishing line information found in 2-D images. In this paper, the vanishing line in the 2-D corridor ceiling image is used to find the 3-D vehicle orientation.

More specifically, we derive the vanishing line of the corridor ceiling by the vanishing points of two sets of parallel lines on the corridor ceiling. It is well known that all vanishing points of the lines in a plane constitute the vanishing line of the plane [16]. Also, as is well known, for a set of parallel lines with line direction (a, b, c) in the CCS, the corresponding vanishing point (u_∞, v_∞) can be derived to be

$$(u_\infty, v_\infty) = f\left(\frac{a}{c}, \frac{b}{c}\right). \tag{6}$$

More details about vanishing points can be found in [16]. Now, given two vanishing points $\mathbf{p}_1$ and $\mathbf{p}_2$ of two coplanar sets of parallel lines, one can compute the line direction of the vanishing line of the plane to be

$$\mathbf{l} = \mathbf{p}_1 - \mathbf{p}_2. \tag{7}$$

B. Vanishing Line of Corridor Ceiling

The line direction of the vanishing line of a corridor ceiling is derived in this section. Two sets of parallel lines on the ceiling with line directions $\mathbf{d}_x = (a_1, b_1, c_1)$ and $\mathbf{d}_z = (a_2, b_2, c_2)$ in the GCS are utilized to derive the desired vanishing points. First, by (2), the line directions of these two sets of lines in the CCS can be obtained. Next, by (6), the corresponding vanishing points can be obtained. Finally, by (7), a formula describing the line direction $\mathbf{d}_{xz}$ of the vanishing line of the corridor ceiling can be found. For example, the derived formula with line directions $\mathbf{d}_x = (1, 0, 0)$ and $\mathbf{d}_z = (0, 0, 1)$ is

$$\mathbf{d}_{xz} = \begin{bmatrix} f(\tan\phi + \cot\phi)\dfrac{\cos\psi}{\cos\theta} \\ f(\tan\phi + \cot\phi)\dfrac{\sin\psi}{\cos\theta} \end{bmatrix}. \tag{8}$$

This is used in the following derivation in this paper.

C. Determination of Vehicle Orientation

The process to detect the vanishing line of the corridor ceiling in an acquired image and then compute its direction (m, n) is as follows. After two sets of parallel lines on the corridor ceiling are extracted from the acquired image, the intersections of the image lines in each line set are computed. The average of the coordinates of all the intersections of the lines in each set is taken as the coordinates of the vanishing point of that line set. Then, by (7), the line direction of the vanishing line in the acquired image, (m, n), can be found.

Since the tilt angle θ and the swing angle ψ of the camera are constants when the vehicle navigates in the corridor, with the detected vanishing line direction (m, n) from the acquired image available, two equations can be established from (8) as follows:

$$m = c_1(\tan\phi + \cot\phi) \tag{9}$$

and

$$n = c_2(\tan\phi + \cot\phi) \tag{10}$$

where $c_1 = f(\cos\psi/\cos\theta)$ and $c_2 = f(\sin\psi/\cos\theta)$, from which the pan angle ϕ of the camera with respect to the GCS can be found to be

$$\phi = \arctan\left(\tfrac{1}{2}\left(c_1^{-1}m \pm \left(c_1^{-2}m^2 - 4\right)^{1/2}\right)\right) \tag{11}$$

or

$$\phi = \arctan\left(\tfrac{1}{2}\left(c_2^{-1}n \pm \left(c_2^{-2}n^2 - 4\right)^{1/2}\right)\right). \tag{12}$$

It is easy to verify that the results calculated by (11) and (12) are exactly the same. Thus, either (11) or (12) can be chosen. In this paper, (11) is selected. Also, two angles are computed by (11) (note the two signs $\pm$ in the equation) which are mutually complemented. The one smaller than 45° is selected as the desired pan angle ϕ of the camera with respect to the GCS. Finally, as defined in Section II-B, the orientation of the vehicle is obtained by transforming this pan angle ϕ through (4).

The computed solution of the vehicle orientation is unique based on the assumption that the pan angle is not greater than 45° in magnitude, as discussed in the following. The lines required are two sets of parallel lines on the corridor ceiling, and each set contains at least two lines. Some parameters should be available in advance, including the intrinsic camera parameters [16], the tilt angle θ and the swing angle ψ of the camera with respect to the corridor, the pan angle ϕ_{vc} of the vehicle with respect to the camera, and the lateral position x_{vc} of the vehicle with respect to the camera, as defined above. The line direction $\mathbf{d}_{xz}$ of the vanishing line of the corridor ceiling can be detected uniquely in the acquired image. Either (11) or (12) can be used alone, because they generate the same output. Both ϕ and (90°–ϕ) satisfy (11) [or (12)], since a pair of complementary angles ϕ and (90°–ϕ) produce the same set $\{\tan\phi, \cot\phi\}$. Rules or other constraints can be imposed here to decide which sign should be selected. However, we use the assumption that the pan angle is not greater than 45° in magnitude. Thus, it can be concluded that a unique solution does exist based on the assumption that the pan angle is not greater than 45°.

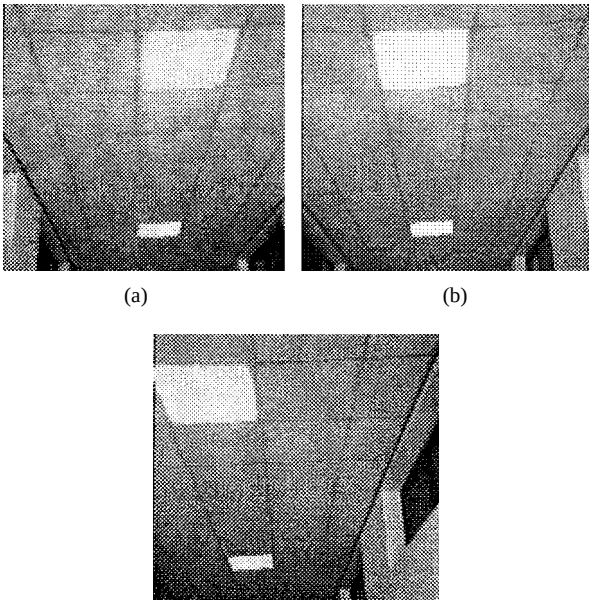

(a) (b) (c)

Fig. 3. Images acquired at different lateral positions. Note that the lines composed of the edges of the ceiling lamps have different slopes. (a) Acquired at left position. (b) Acquired in the middle position. (c) Acquired at right position.

IV. Detection of Lateral Position of Vehicle by Image Line Slopes

In order to keep the vehicle navigating safely in the right parallelepiped corridor, the lateral position of the vehicle must be known. In this paper, the slopes of the image lines pointing forward on the ceiling are utilized to compute the lateral position of the vehicle. Such a method is based on the following observation. When we move left or right horizontally and look at the lines pointing forward on the ceiling, as shown in Fig. 3, we can see these lines varying in their line slopes. From this observation, we consider that the information of such image line slopes provides a certain hint to the lateral position of the vehicle. Accordingly, in the following, the line slopes in the

ICS of known lines in the GCS are derived first. The derivation is done step by step, namely, from the GCS, through the CCS, to the ICS. Then, a formula to compute the lateral position of the vehicle is derived.

A. Image Line Slopes of 3-D Lines

Consider a line L in the GCS represented by a set of points, which passes through the point (p_x, p_y, p_z) and has the line direction (d_x, d_y, d_z)

$$L = \{(x, y, z) | (x, y, z) = (p_x, p_y, p_z) + \lambda(d_x, d_y, d_z) \text{ for some real value } \lambda\}. \quad (13)$$

By (1) and (2), the set of points which represents the corresponding line L' in the CCS can be written as follows:

$$L' = \{(x', y', z') | (x', y', z') = (p_{x'}, p_{y'}, p_{z'}) + \lambda(d_{x'}, d_{y'}, d_{z'}) \text{ for some real value } \lambda\} \quad (14)$$

where

$$(p_{x'}, p_{y'}, p_{z'}) = (p_x - x_d, p_y - y_d, p_z - z_d)\mathbf{T}_\phi\mathbf{T}_\theta\mathbf{T}_\psi, \quad (15)$$

and

$$(d_{x'}, d_{y'}, d_{z'}) = (d_x, d_y, d_z)\mathbf{T}_\phi\mathbf{T}_\theta\mathbf{T}_\psi. \quad (16)$$

By (3), the set of points which represents the corresponding line L'' in the ICS can be written as follows:

$$L'' = \left\{(u, v) | (u, v) = f\left(\frac{p_{x'} + \lambda d_{x'}}{p_{z'} + \lambda d_{z'}}, \frac{p_{y'} + \lambda d_{y'}}{p_{z'} + \lambda d_{z'}}\right) \text{ for some real value } \lambda\right\}. \quad (17)$$

The line direction $\mathbf{d}''$ of the image line L'' can be derived by computing the vector connecting two arbitrary points on L''. For this, $\lambda = 0$ and $\lambda = 1$ are chosen to yield two points, resulting in the following line direction $\mathbf{d}''$:

$$\mathbf{d}'' = \frac{f}{p_{z'}(p_{z'} + d_{z'})}(p_{x'}d_{z'} - p_{z'}d_{x'},\ \ p_{y'}d_{z'} - p_{z'}d_{y'}). \quad (18)$$

Finally, the line slope θ'' can be easily found accordingly as follows:

$$\theta'' = \arctan\left(\frac{p_{y'}d_{z'} - p_{z'}d_{y'}}{p_{x'}d_{z'} - p_{z'}d_{x'}}\right). \quad (19)$$

B. Determination of Lateral Position of Vehicle by Image Line Slopes

One of the lines pointing forward on the ceiling in the GCS is chosen for deriving the lateral position of the vehicle. For convenience, we choose the one which passes through a specific point $(x_l, y_l, 0)$ on the ceiling and has line direction $(0, 0, 1)$. Also, suppose that the camera is located at $(x_l + \Delta x_c, y_c, 0)$. Note that Δx_c is the lateral position of the camera with respect to line L, and the camera orientation with respect to the GCS is obtained in Section III.

Under the above assumptions, by (13) and (14), a point $(p_{x'}, p_{y'}, p_{z'})$ on line L' and the direction $(d_{x'}, d_{y'}, d_{z'})$ of L' in the CCS can be computed to be

$$(p_{x'}, p_{y'}, p_{z'}) = \begin{pmatrix} -\Delta x_c\ \mathrm{r}_{11} + (y_l - y_c)\ \mathrm{r}_{21} \\ -\Delta x_c\ \mathrm{r}_{12} + (y_l - y_c)\ \mathrm{r}_{22} \\ -\Delta x_c\ \mathrm{r}_{13} + (y_l - y_c)\ \mathrm{r}_{23} \end{pmatrix}^{\mathrm{T}} \quad (20)$$

and

$$(d_{x'}, d_{y'}, d_{z'}) = (\mathrm{r}_{31}, \mathrm{r}_{32}, \mathrm{r}_{33}) \quad (21)$$

respectively, where r_{ij} are defined by the following equation for brevity of representation:

$$\begin{pmatrix} \mathrm{r}_{11} & \mathrm{r}_{12} & \mathrm{r}_{13} \\ \mathrm{r}_{21} & \mathrm{r}_{22} & \mathrm{r}_{23} \\ \mathrm{r}_{31} & \mathrm{r}_{32} & \mathrm{r}_{33} \end{pmatrix} = \mathbf{T}_\phi\mathbf{T}_\theta\mathbf{T}_\psi. \quad (22)$$

Now, by (19)–(22), we can obtain $\tan\theta''$ as follows:

$$\tan\theta'' = \frac{\Delta x_c(\mathrm{r}_{13}\mathrm{r}_{32} - \mathrm{r}_{12}\mathrm{r}_{33}) + (y_l - y_c)(\mathrm{r}_{22}\mathrm{r}_{33} - \mathrm{r}_{23}\mathrm{r}_{32})}{\Delta x_c(\mathrm{r}_{13}\mathrm{r}_{31} - \mathrm{r}_{11}\mathrm{r}_{33}) + (y_l - y_c)(\mathrm{r}_{21}\mathrm{r}_{33} - \mathrm{r}_{23}\mathrm{r}_{31})}. \quad (23)$$

Thus, by (23), Δx_c, the lateral position of the camera with respect to the line, can be solved to be

$$\Delta x_c = (y_l - y_c)\frac{(\mathrm{r}_{22}\mathrm{r}_{33} - \mathrm{r}_{23}\mathrm{r}_{32}) - (\mathrm{r}_{21}\mathrm{r}_{33} - \mathrm{r}_{23}\mathrm{r}_{31})\tan\theta''}{(\mathrm{r}_{12}\mathrm{r}_{33} - \mathrm{r}_{13}\mathrm{r}_{32}) - (\mathrm{r}_{11}\mathrm{r}_{33} - \mathrm{r}_{13}\mathrm{r}_{31})\tan\theta''}. \quad (24)$$

Finally, the lateral position of the vehicle with respect to the line can be computed by transforming the result of (24) by (5). The uniqueness of the computation of the vehicle lateral position can be easily verified, since all parameters involved in (24) are unique.

V. Experimental Results and Discussions

In the following, the details of some simulations and the results are described to verify the correctness of the derived formulas. Next, the employed image processing techniques and some experimental results on real images are shown to prove the feasibility of the proposed approach. Then, some simulations are described to find the error in larger ranges of vehicle orientations. Finally, limitations and complexity of the proposed approach are discussed.

Simulations have been done with noise-free data. The computation results are accurate. A global coordinate system was created as the GCS and two coplanar sets of parallel lines were constructed in the GCS. The position and the orientation of the camera were randomly selected in the GCS. It is assumed that the location of the vehicle is identical to that of the camera. The equations of the two sets of lines in the GCS were transformed into the ICS. The derived formulas were used to compute the vehicle orientation and lateral position, which were then compared with the correct data. The relative error of the vehicle orientation and lateral position are both zero for all tested data.

In the experiments with real images, the corridor ceilings, as shown in Fig. 3, were imaged. In order to simplify the experiments, the camera orientation and the lens center were

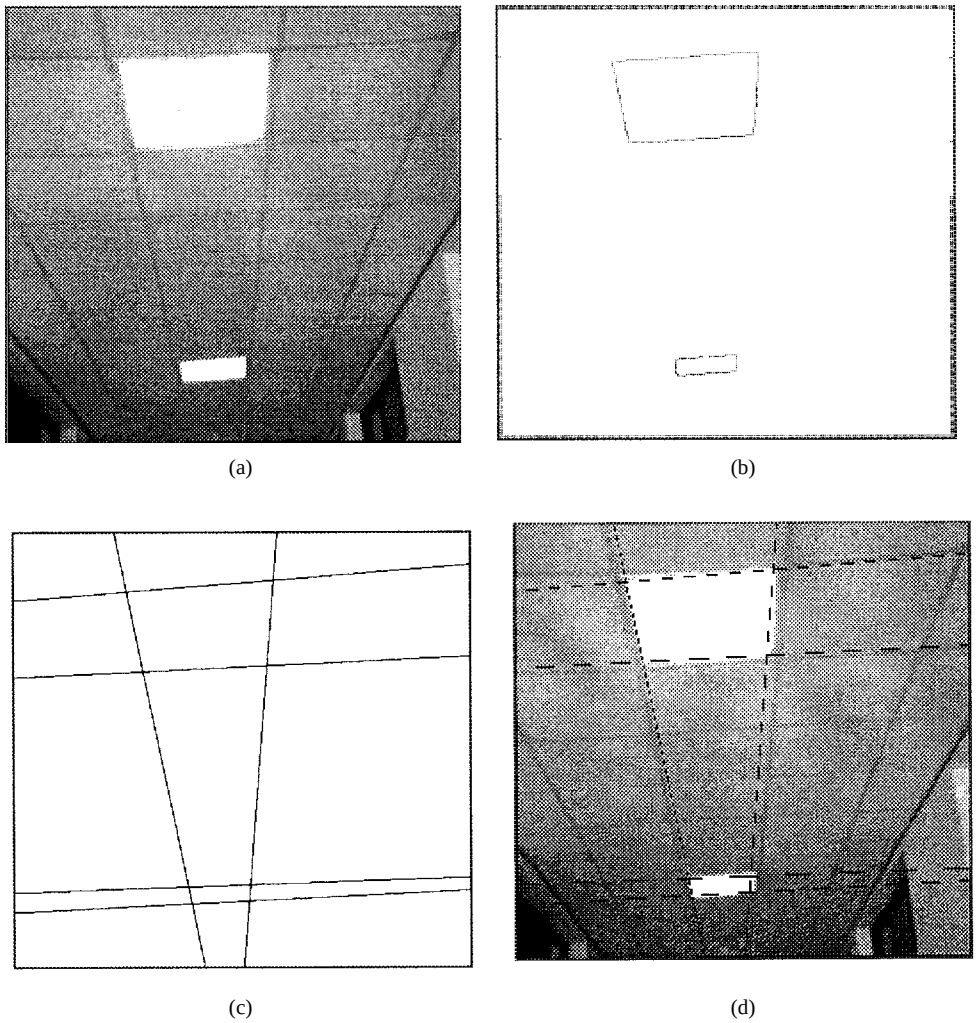

Fig. 4. An image processing result. (a) Original image. (b) Result of edge detection. (c) Result of line detection. (d) Image processing result shown on original image.

treated as the vehicle orientation and position, respectively, and the camera was supported by a tripod. Two sets of parallel lines composed of lamp edges in the corridor ceiling image were extracted. The reason why the algorithm was calculated based on the edges of the lamps is that such data are less disturbed by other light sources at the intersections or locations near corridor exits. The employed image processing techniques include edge [17] detection and line detection. The Hough transform [18] was applied to the resulting edge points to detect candidate lines. These candidate lines were then merged into a smaller number of lines if they have similar line slopes and if the center points of the corresponding line segments on the acquired image are close enough. The merged lines were further improved by least-square-error line fitting. The detected image lines can be easily divided into two sets of lines, and the detection of the desired elements for the proposed approach was finished. An example of the image processing results is shown in Fig. 4, in which the reason why the edge lines do not coincide with the boundary of the lamps is that the sampling was made coarser in order to speed up the computation process.

The computed results were compared with the correct data to derive the errors. Two kinds of error were derived to show the goodness of the experimental results. One is the relative error of computed vehicle orientations compared with the manual measurements. The manual measurement was done by adjusting the camera to the direction of pointing forward in the corridor. It means that only zero degree was tested here. The reason is to avoid the error of the manual measurement, since the orientation of the camera is difficult to measure by hand. Larger ranges of nonzero degrees were tested by conducting simulations. The experimental results with real images can be found in Table I. The average error is about 1.23°. The other kind of error is the relative error of the computed lateral positions of the vehicle compared with the manual measurements. Here, the manual measurement was done by measuring the lateral distances between the ceiling lines and one leg of the tripod with a ruler, and the lateral distance between the leg of the tripod and the camera was estimated by a camera calibration technique [15]. The result is shown in Table II. It is can be seen that the proposed approach can find different lateral positions of the vehicle according to the images acquired at different positions. The variation of the

TABLE I
EXPERIMENTAL RESULTS FOR VEHICLE ORIENTATION

	computed vehicle orientation (degree)	measured vehicle orientation (degree)	relative error (degree)
1	0.9035	0.0000	0.9035
2	0.0000	0.0000	0.0000
3	0.0000	0.0000	0.0000
4	0.7682	0.0000	0.7682
5	-2.3792	0.0000	2.3792
6	1.0943	0.0000	1.0943
7	1.7672	0.0000	1.7672
8	-1.5211	0.0000	1.5211
9	-1.4739	0.0000	1.4739
10	2.4176	0.0000	2.4176

TABLE II
EXPERIMENTAL RESULTS FOR VEHICLE LATERAL POSITION

	computed vehicle lateral position (to left line, to right line) (cm, cm)	manual measurement (to left line, to right line) (cm, cm)	relative error (at left line, at right line) (cm, cm)
1	(-6.8281, -65.7985)	(-5.9681, -65.9681)	(0.8600, 0.1696)
2	(-6.8281, -62.3204)	(-5.9681, -65.9681)	(0.8600, 3.6478)
3	(-6.8281, -62.2587)	(-5.9681, -65.9681)	(0.8600, 3.7094)
4	(14.9870, -41.8937)	(14.0319, -45.9681)	(0.9551, 4.0744)
5	(11.9690, -41.9332)	(14.0319, -45.9681)	(2.0629, 4.0349)
6	(11.9669, -45.3374)	(14.0319, -45.9681)	(2.0650, 0.6307)
7	(34.0329, -22.5979)	(34.0319, -25.9681)	(0.0010, 3.3702)
8	(37.3237, -22.5852)	(34.0319, -25.9681)	(3.2918, 3.3829)
9	(37.4285, -22.6455)	(34.0319, -25.9681)	(3.3966, 3.3226)
10	(77.4847, 14.9491)	(74.0319, 14.0319)	(3.4528, 0.9172)

calculation results is due to the noise produced in the camera at each sampling time. The average error is about 2.25 cm. The accuracy of the proposed approach is kept between 0°–2.5° for orientation, and between 0.001–4.1 cm for lateral position. It is similar to the accuracy described in other approaches [1], [3], [7]. For the requirement of the vehicle location precision in the application of vehicle navigation in corridors, both of the two kinds of errors show that the computation results are acceptable. For each acquired image, the processing time is about 0.5 s. The estimation is based on a personal computer with a CPU of Pentium 100 MHz. By improving the software efficiency and the hardware equipment, even faster speed can be attained.

Some simulations were performed to find the error in larger ranges of vehicle orientations. The parameters in the experiments with real images were all adopted in the simulations. The errors of the vehicle orientation and lateral position were computed at different vehicle orientations ranging from $+45°$ to $-45°$ and at different vehicle lateral positions ranging from -400 to $+400$ cm. The perspective projection of the edge points of the lamps was computed and perturbed. The perturbation was performed by adding normally distributed noise to both the u and v coordinates of each edge point of the lamps with a mean of zero and a specified standard deviation. Then, the least-square-error fitting was used to fit the line equations. For each specific vehicle orientation and lateral position, 100 perturbation data sets were generated randomly, and the average error was calculated. The result is shown in Fig. 5. It can be seen that all the errors are acceptable.

Limitations of the proposed approach are now discussed. Two orthogonal sets of parallel lines should be available on the ceiling and each set contains at least two lines, and it is necessary that one set of parallel lines should have the same direction with which the vehicle navigates. However, the process described in Section III can be easily extended to the case with two nonorthogonal sets of parallel lines. Based on the simulation results shown in Fig. 5, it can be seen that the range of the orientation in which localization can be operated is the range of the orientation of the vehicle in which the two sets of parallel lines are within the view area of the camera, and the range of the lateral position in which localization can be operated is the range of the lateral position of the vehicle in which the two sets of parallel lines are within the view area of the camera.

The complexity of the proposed approach is now analyzed. Let m be the number of lines detected. The complexity of

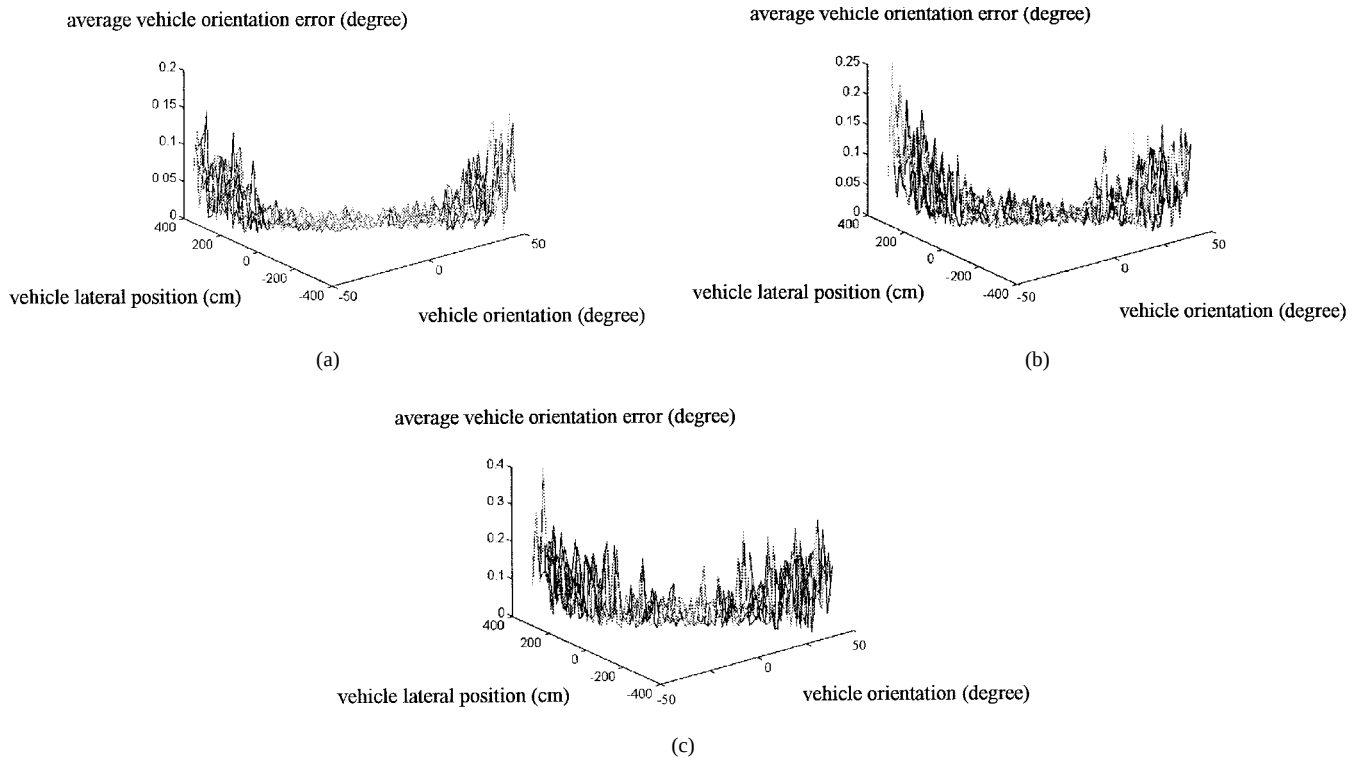

Fig. 5. Plots of the average vehicle lateral position error (degree) versus the vehicle lateral position and orientation. (a) Noise level is 0.5 pixel. (b) Noise level is 1.0 pixel. (c) Noise level is 2.0 pixel.

vanishing line detection is $O(m^2)$. Although it is quadratic, practically, the value m is rather small. After the vanishing line is detected, only formula computation is needed, and it takes $O(1)$. In [1], the complexity is $O(m^2)$ for the computation of the Kalman gain which is used to update the robot location. Then, it costs $O(m)$ to compute the robot location. In [4], the complexity of robot location is $O(m)$ after 3-D-to-2-D line correspondence is established. However, the complexity of 3-D-to-2-D line correspondence establishment is higher than $O(m^4)$. From the above observation, it can be seen that formula computation in our approach has lower complexity, and the use of vanishing line information avoids the complicated 3-D-to-2-D line correspondence problem.

VI. Conclusions

In this paper, an approach to vehicle localization in corridors by computer vision techniques has been proposed, based on the basic idea of treating corridors as a combination of right parallelepipeds. The orientation and lateral position of a vehicle are obtained by derived formulas using single images. The corridor ceiling edges are chosen as the information source due to their stable property. The orientation of the vehicle is derived by the vanishing line of the ceiling edge lines in the image, and the lateral position of the vehicle is computed by the edge line slopes in the image. Only computation of some analytic formulas is needed, which speeds up the estimation process. Low hardware cost is also guaranteed, since only one camera is required. No information of the dead-reckoning system is required. Acceptable experimental results have been obtained both by simulation and by testing real corridor images. Based on the proposed method, future work may be directed to developing systems not only for guiding the vehicle in a straight corridor, but also for navigating the vehicle at intersections, achieving obstacle avoidance, and so on.

Acknowledgment

The authors gratefully appreciate the suggestions of the anonymous reviewers.

References

[1] A. D. L. Escalera, L. Moreno, M. A. Salichs, and J. M. Armingol, "Continuous mobile robot localization by using structured light and a geometric map," *Int. J. Syst. Sci.*, vol. 27, no. 8, pp. 771–782, 1996.
[2] A. Curran and K. J. Kyriakopoulos, "Sensor-based self-localization for wheeled mobile robots," *J. Robot. Syst.*, vol. 12, no. 3, pp. 163–176, 1995.
[3] P. S. Lee, Y. E. Shen, and L. L. Wang, "Model-based location of automated guided vehicles in the navigation sessions by 3D computer vision," *J. Robot. Syst.*, vol. 11, no. 3, pp. 181–195, 1994.
[4] R. Talluri and J. K. Aggarwal, "Mobile robot self-location using model-image feature correspondence," *IEEE Trans. Robot. Automat.*, vol. 12, pp. 63–77, Feb. 1996.
[5] H. L. Chou and W. H. Tsai, "A new approach to robot location by house corners," *Pattern Recognit.*, vol. 19, no. 6, pp. 439–451, 1986.
[6] S. Atiya and G. D. Hager, "Real-time vision-based robot localization," *IEEE Trans. Robot. Automat.*, vol. 9, pp. 785–800, Dec. 1993.
[7] A. Gilg and G. Schmidt, "Landmark-oriented visual navigation of a mobile robot," *IEEE Trans. Ind. Electron.*, vol. 41, pp. 392–397, Aug. 1994.
[8] L. Trassoudaine, S. Jouannin, J. Alizon, and J. Gallice, "Tracking systems for intelligent road vehicles," *Int. J. Syst. Sci.*, vol. 27, no. 8, pp. 731–743, 1996.
[9] N. Amano, H. Hashimoto, and M. Higashiguchi, "Estimation of vehicle position based on projective function using the sequence of a 2D image," *Int. J. Syst. Sci.*, vol. 27, no. 8, pp. 783–788, 1996.

[10] N. Ayache and O. D. Faugeras, "Maintaining representations of the environment of a mobile robot," *IEEE Trans. Robot. Automat.*, vol. 5, pp. 804–819, Dec. 1989.
[11] D. J. Kriegman, E. Triendl, and T. O. Binford, "Stereo vision and navigation in buildings for mobile robots," *IEEE Trans. Robot. Automat.*, vol. 5, pp. 792–803, Dec. 1989.
[12] P. W. Lux and C. H. Schaefer, "Range imaging for autonomous navigation of robotic land vehicles," *Signal Process.*, vol. 22, no. 3, pp. 299–311, Mar. 1991.
[13] L. S. Davis, "Visual navigation at the University of Maryland," *Robot. Autonomous Syst.*, vol. 7, no. 2-3, pp. 99–111, Aug. 1991.
[14] E. T. Baumgartner and S. B. Skaar, "An autonomous vision-based mobile robot," *IEEE Trans. Automat. Contr.*, vol. 39, pp. 493–502, Mar. 1994.
[15] L. L. Wang, P. Y. Ku, and W. H. Tsai, "Model-based guidance by the longest common subsequence algorithm for indoor autonomous vehicle navigation using computer vision," *Automat. Construction*, vol. 2, pp. 123–137, 1993.
[16] R. M. Haralick and L. G. Shapiro, *Computer and Robot Vision.* Reading, MA: Addison-Wesley, 1993.
[17] D. E. Pearson and J. A. Robinson, "Visual communication at very low data rates," *Proc. IEEE*, vol. 73, pp. 795–812, Apr. 1985.
[18] R. C. Gonzalez and R. E. Woods, *Digital Image Processing.* Reading, MA: Addison-Wesley, 1992.
[19] Chen and Jiang, "3D camera calibration using vanishing point concept," *Pattern Recognit.*, vol. 24, no. 1, pp. 57–67, 1991.

Zhi-Fang Yang was born in Taipei, Taiwan, R.O.C., in 1971. She received the B.S. degree in 1993 from National Chiao Tung University, Hsinchu, Taiwan, R.O.C., where she is currently working towards the Ph. D. degree

Since August 1993, she has been a Research Assistant with the Computer Vision Laboratory, Department of Computer and Information Science, National Chiao Tung University. Her current research interests include pattern recognition, image processing, computer vision, and autonomous vehicle navigation.

Wen-Hsiang Tsai (S'78–M'79–SM'91) was born in Taiwan, R.O.C., in 1951. He received the Ph.D. degree in electrical engineering from Purdue University, West Lafayette, IN, in 1979.

In November 1979, he joined the faculty of National Chiao Tung University, Hsinchu, Taiwan, R.O.C., where he has been a Department Head, the Associate Director of the Microelectronics and Information System Research Center, and the Dean of General Affairs. He is currently a Professor and the Dean of Academic Affairs. He has also served as a Consultant to several major research and development institutions in Taiwan. He has been the Editor of several academic journals, including *Computer Quarterly* (now *Journal of Computers*), *Proceedings of the National Science Council*, *International Journal of Pattern Recognition and Artificial Intelligence*, and *Journal of Information Science and Engineering*. He is currently the Editor of the *Journal of Chinese Engineers* and the Editor-in-Chief of the *Journal of Information Science and Engineering*. His major research interests include image processing, pattern recognition, computer vision, neural networks, and Chinese information processing. He has authored more than 190 published academic papers, including 83 journal papers.

Dr. Tsai is the recipient of several awards, including one Distinguished Research Award, four Outstanding Research Awards, and one Special Research Project Award from the National Science Council, Taiwan, R.O.C., in 1987 and 1998. He was the recipient of the 13th Annual Best Paper Award from the Pattern Recognition Society. He is a member of the Chinese Image Processing and Pattern Recognition Society, the Medical Engineering Society of the Republic of China, and the International Chinese Computer Society.